In Vitro Assembly and Structure of Trichocyte Keratin Intermediate Filaments: A Novel Role for Stabilization by Disulfide Bonding

He Wang,* David A.D. Parry,‡ Leslie N. Jones,§ William W. Idler,* Lyuben N. Marekov,* and Peter M. Steinert*

*Laboratory of Skin Biology, National Institute of Arthritis and Musculoskeletal and Skin Diseases, National Institutes of Health, Bethesda, Maryland 20892; ‡Institute of Fundamental Sciences, Massey University, Palmerston North 5301, New Zealand; and §Commonwealth Scientific and Industrial Research Organisation, Division of Wool Technology, Belmont, Victoria 3216, Australia

Abstract. Intermediate filaments (IF) have been recognized as ubiquitous components of the cytoskeletons of eukaryotic cells for 25 yr. Historically, the first IF proteins to be characterized were those from wool in the 1960s, when they were defined as low sulfur keratins derived from "microfibrils." These proteins are now known as the type Ia/type IIa trichocyte keratins that constitute keratin IF of several hardened epithelial cell types. However, to date, of the entire class of >40 IF proteins, the trichocyte keratins remain the only ones for which efficient in vitro assembly remains unavailable. In this paper, we describe the assembly of expressed mouse type Ia and type IIa trichocyte keratins into IF in high yield. In cross-linking experiments, we document that the alignments of molecules within reduced trichocyte IF are the same as in type Ib/IIb cytokeratins. However, when oxidized in vitro, several intermolecular disulfide bonds form and the molecular alignments rearrange into the pattern shown earlier by x-ray diffraction analyses of intact wool. We suggest the realignments occur because the disulfide bonds confer substantially increased stability to trichocyte keratin IF. Our data suggest a novel role for disulfide bond cross linking in stabilization of these IF and the tissues containing them.

Key words: intermediate filaments • trichocyte keratins • cytokeratins • disulfide bonding • molecular organization

Introduction

By the late 1970s, it had become clear that intermediate filaments (IF)[1] are ubiquitous components of eukaryote cells. Together with actin-containing microfilaments and tubulin-containing microtubules, the IF form a complex, dynamic, interactive cytoskeleton in almost all cells. We now know that IF are very complex, as at least 50 different IF proteins exist (Fuchs and Weber, 1994; Parry and Steinert, 1995, 1999; Herrmann and Aebi, 1998).

In retrospect, cytologists had visualized IF in wool and wool follicle cells for several decades before the 1970s. The IF form 8–10-nm wide "microfibrils," embedded in a densely staining matrix. Further, the first IF proteins to be studied rigorously at the biochemical/molecular level were the "low sulfur" α-helical proteins extracted from wool (for review, see Fraser et al., 1972; Woods and Inglis, 1984; Herrling and Sparrow, 1991). Now we know that there are ~20 different trichocyte keratin chains in human, divided into type Ia and type IIa families of ~10 members each (Langbein et al., 1999). They are predominantly expressed in "hard" keratinizing tissues such as in the cortical cells of hair and nails, the filiform ridges of the tongue, etc. These keratins contained ~5% cysteine residues, and are thought to be disulfide bonded to form a hardened rigid structure important for the biomechanical properties of wool and related tissues (Fraser et al., 1988). There are also another 20 or so type Ib and IIb cytokeratins that are widely expressed in many different epithelia. In addition, there are ~10 more types III–VI IF chains.

As the trichocyte IF are well oriented in wool fibers and quills, they were readily amenable to x-ray diffraction analyses, from which a number of structural features were adduced (Fraser and MacRae, 1983, 1985; Fraser et al., 1964, 1986; reviewed in Fraser et al., 1972; Parry and Steinert, 1995, 1999). Notably, the IF were shown to be composed of arrays of 47-nm-long coiled-coil heterodimer molecules. It was shown that the second step in hierarchical structural order was the antiparallel alignment of a pair of such molecules in one of three modes (now termed A_{11}, A_{22}, and A_{12}) that differ in the degree to which the molecules are overlapped

Address correspondence to Peter M. Steinert, Building 6 Room 425, NIAMS, NIH, Bethesda, MD 20892-2752. Tel.: (301) 496-1578. Fax: (301) 402-2886. E-mail: pemast@helix.nih.gov

[1]*Abbreviations used in this paper:* Cu-P, copper II-phenanthroline; DST, disulfosuccinimidyl tartrate; IF, intermediate filament; TCEP, tris(2-carboxyethyl)phosphine hydrochloride.

or aligned. The dimensions of these alignments allowed the prediction of a fourth alignment mode, A_{CN}, in which two parallel molecules in the same axial row within a trichocyte keratin IF have an apparent gap of ~1 nm (Parry, 1995, 1996).

We and others have devised methods for the assembly of cytokeratins or types III, IV, and VI IF chains in vitro (Steinert et al., 1976, 1999; Hatzfeld and Franke, 1985; Herrmann et al., 1996). This has provided an alternative tool with which to determine the packing of molecules within IF. Cross-linking experiments revealed that A_{11}, A_{22}, and A_{12} antiparallel molecular alignments are also present, but in comparison with the trichocyte keratin IF of wool, the A_{11} mode is shifted so that there is an approximately eight-residue (1-nm) overlap in the A_{CN} mode instead (Steinert et al., 1993a,b,c, 1999). This overlap region encompasses the 10–15 residue highly conserved helix initiation and helix termination sequences at the extreme ends of the 1A and 2B rod domain segments, respectively. These overlap regions are of notable importance because mutations leading to inappropriate amino acid substitutions in cytokeratins cause a variety of epithelial diseases (reviewed in Korge and Krieg, 1996; Irvine and McLean, 1999).

A major question thus arises as to why the structures of cytokeratin and trichocyte keratin IF appear to be different from each other. Heretofore, it has not been possible to obtain sufficiently well-oriented specimens of cytokeratins (or other types of IF) to perform x-ray diffraction analyses as done for wool. Also, although preliminary reports have appeared (Heid et al., 1988; Winter et al., 1997), conditions for efficient assembly of trichocyte keratins into native-type IF in vitro have not been described to allow cross-linking experiments. In this paper, we have expressed representative types Ia and IIa mouse keratin chains, and describe their efficient assembly in vitro using strongly reducing conditions. Further, we show that the molecular parameters for the alignment of neighboring molecules of reduced trichocyte keratin IF are the same as for cytokeratins. However, we show that, upon oxidation of cysteine residues, molecular realignments occur in trichocyte keratin IF, and a gap forms in the A_{CN} mode, yielding an organization similar to that seen by x-ray diffraction analyses of mature wool. These data suggest that disulfide bonding plays a novel role in the molecular organization and stabilization of IF.

Materials and Methods

Expression and Purification of Mouse Types Ia and IIa Trichocyte Keratin Chains

Hair follicles from neonatal BALB/c mice (<2 d of age) were isolated and purified as described previously (Weinberg et al., 1993), from which total RNA was recovered using the Trizol method (Life Technologies). Using published cDNA sequences encoding types Ia (Bertolino et al., 1988) and IIa (Yu et al., 1991) mouse hair keratins, we generated PCR primers to amplify the full-length coding sequences coupled with restriction enzyme sites at the 5′ and 3′ ends for subsequent insertion into the NdeI/BamH1 sites, respectively, of the pET11a vector (Novagen). The constructs were transfected into the bacterial strain BL21 (DE3). Bacteria were grown at 37°C up to an OD_{600} = 0.6 in 1 liter of Luria broth supplemented with 50 μg/ml carbenicillin and 20 ml of 50% glucose for 3 h, followed by induction with 1 mM IPTG for 3 h. Analysis of bacterial pellets revealed that the keratins were highly enriched in inclusion bodies. These were dissolved in gel sample loading buffer containing 1% SDS and 5 mM [Tris(2-carboxyethyl)-phosphine-HCl] (TCEP) (Pierce Chemical Co.), clarified by centrifugation at 15,000 *g*, and resolved on 3-mm-thick 10% slab PAGE gels. The desired bands were cut out, eluted overnight into a buffer of 50 mM Tris-HCl, pH 8.0, 2 mM EDTA, 5 mM TCEP, and 0.2% SDS, and stored frozen (−80°C) in this solution until further use. In this way, proteins were recovered in >95% purity (see Fig. 3). Protein concentrations were ascertained by amino acid analysis after acid hydrolysis.

Samples of adult BALB/c mouse hair were degreased by washing in chloroform/methanol (50:50), dried, and extracted in a buffer of 50 mM Tris-HCl, pH 9.0, 2 mM EDTA, 5 mM TCEP, and 0.1% SDS for 16 h at 23°C (1 g/100 ml). After filtration and centrifugation at 15,000 *g*, aliquots were resolved on slab gels. Major bands corresponding to the families of types II (~55 kD) and I (~45 kD) trichocyte keratins were cut out and eluted into SDS buffer as above.

IF Assembly In Vitro

Equimolar mixtures of the purified type Ia/IIa chains were mixed in SDS solution and SDS was removed by ion-pair extraction (Konigsberg and Henderson, 1983). Pellets were redissolved (either 50 or 500 μg/ml) in a buffer of 10 mM Tris-HCl, pH 9.0, 9.5 M urea, 2.5 mM EDTA, and 5 mM TCEP, which had been degassed with house vacuum (≈5 mm of pressure) and restored in a N_2 atmosphere. Solutions were then dialyzed for 1 h each in degassed/N_2-restored buffers containing 10 mM Tris-HCl, pH 8.0, 2.5 mM EDTA, and 5 mM TCEP, and with decreasing urea concentrations of 6, 4, and 2.5 M urea. Final 4-h dialyses were performed against the same degassed/N_2-restored buffers containing no urea and either 25 mM NaCl [= low (L) salt buffer], 175 mM NaCl [= high (H) salt buffer], or 175 mM NaCl with 5 mM $MgCl_2$. IF samples to be used for cross-linking experiments were equilibrated into triethanolamine buffers instead. Yields of protein in IF particles were determined in 50-μl aliquots after centrifugation at either 15,000 or 100,000 *g* for 30 min in an AirFuge (Beckman Coulter), followed by measurement of the $A_{280\ nm}$ absorbance of the supernatants. Samples of IF particles were visualized by electron microscopy after negative staining with 0.7% aqueous uranyl acetate on carbon-coated holey film grids. In some cases, samples were equilibrated in buffers that had not been degassed, or contained 5 mM dithiothreitol instead of TCEP. In other experiments, samples in L buffer were made to 175 mM NaCl by addition of 1 M salt and examined by electron microscopy in 10–15 s.

Cross-Linking Procedures with Disulfosuccinimidyl Tartrate

Cross linking was done in triethanolamine buffers with 0.4 mM disulfosuccinimidyl tartrate (DST) as described previously (Steinert et al., 1993a,b,c). Reactions containing 50–100 nmol of equimolar amounts of the trichocyte Ia/IIa chains (≤50 μg/ml protein concentration) were reacted for 30 min at 23°C and stopped by quenching with 0.1 M NH_4HCO_3 (final concentration). Proteins were then alkylated with 25 mM iodoacetamide for 4 h at 23°C to modify all cysteine-SH groups. The excess NH_4^+ served to quench modification of the ε-NH_2 group of lysines. Excess iodoacetamide was destroyed with 30 mM DTT. Samples were next resolved on 3.75–7.5% SDS-PAGE gels. In preparative experiments, 3-mm-thick slab gels were used with Tricine buffers. The bands were cut out and eluted as above. In this way, we recovered 1–10 nmol (based on heterodimer size of 95 kD) amounts of oligomers containing one, two, four, and eight molecules.

Cross linking with DST in concentrated urea solutions was done with 25 mM reagent as before using protein concentrations of ≤50 μg/ml (Steinert et al., 1999).

Oxidative Cross Linking with the Copper II-Phenanthroline Reagent

Using an enclosed N_2 atmosphere, equimolar mixtures of the Ia/IIa chains in degassed/N_2 restored triethanolamine L buffer at ≤50 μg/ml were freed of TCEP by passage through a 5 × 1 cm Sephadex G-25 column, and then oxidized with the copper II-phenanthroline (Cu-P) reagent as described (Baird and Hammes, 1976) for 2–8 h at 23°C. The efficiency of oxidation (that is, loss of free–SH groups) was measured by use of iodoacetamide as above. In some experiments, samples were immediately resolved on 3-mm-thick slab gels in the absence of reducing agent, and the desired bands were cut out and eluted as above into buffer not containing TCEP. In other experiments, the oxidized products were first cross linked with DST as above and oligomers were resolved from slab gels.

Separation and Sequencing of Peptides

For analysis of oxidized peptides, proteins were freed of SDS by ion pair extraction, redissolved in degassed/N_2 restored 0.1 M *N*-ethylmorpholine acetate, pH 8.3, and digested to completion with trypsin (bovine, sequencing grade; Sigma-Aldrich) in a N_2 atmosphere using 2% (wt) for 6 h at 37°C, followed by another 1% for 16 h. For DST–cross-linked peptides, after removal of SDS, the proteins were first cleaved with CNBr (Steinert et al., 1993a).

Peptides were resolved by HPLC using a 150 × 2 mm C_{18} column (Phenomenex) with a 2-h non-linear gradient from 10–90% acetonitrile, and as done previously (Steinert et al., 1999). For DST–cross-linked or oxidized samples, comparisons of profiles of samples before and after reaction revealed several shifted and/or new tryptic peptide peaks that were collected for sequencing as described previously (Steinert et al., 1999). The PTH derivative of the *S*-carboxymethyl amide derivative of cysteine eluted near PTH-Glu. By sequencing, it was possible to identify all of the Lys residues involved in DST cross links, and most of the Cys residues involved in Cu-P-induced disulfide bond cross links.

Determination of Axial Parameters in Trichocyte IF

Most of the cross links between juxtaposed Lys and Cys residues could be assigned by simple inspection to one of four modes: some common and abundant cross links were due to intramolecular links between the trichocyte type Ia/IIa chains of the heterodimer; three other modes were due to intermolecular links of the A_{11}, A_{22}, and A_{12} type, as found before (Steinert et al., 1993a,b,c, 1999). The data were used in least squares analyses to refine the six parameters needed to determine the axial properties of the IF.

Results

Purification of Mouse Trichocyte Types Ia and IIa Chains

The two keratin proteins were purified as described in Materials and Methods and were recovered at >90% homogeneity (data not shown; see Fig. 3). The yields of purified proteins were 0.5–1 mg/liter of bacterial growth medium.

Assembly of Trichocyte Keratins into IF In Vitro Is Critically Dependent on Efficient Reducing Conditions

A previous study has demonstrated that human trichocyte keratins assemble into IF in neutral buffers of near-physiological salt concentration (Winter et al., 1997). Here, we varied all parameters to optimize IF yields and quality, using as criteria: (a) maximal yield of protein that could be pelleted at 100,000 *g* in the Airfuge, and (b) optimal quality of IF structures assembled with minimal obvious particulate or unassembled protein, as visualized by electron microscopy after negative staining. We verified here that optimal assembly occurred at pH 7.5–8.0 and with total ionic strengths between 150 and 200 mM. Using a buffer of 10 mM Tris-HCl, pH 8.0, 175 mM NaCl, and 2.5 mM EDTA (=H buffer) containing 5 mM DTT as the reducing reagent, pelletable yields varied between 30 and 50%, the visible IF particles were short (0.2–0.5 μm), and fields were heavily populated by particulate matter (Fig. 1 A). However, when we used degassed/N_2-restored buffers containing 5 mM DTT, yields were 70–80% and the visible quality of IF fields, although not IF lengths, greatly improved (Fig. 1 B). Moreover, when DTT was replaced by 5 mM TCEP as a superior reducing reagent in degassed/N_2-restored buffers, IF yields were routinely >90% (at 0.4–0.5 mg/ml), and the IF were smooth-walled fairly uniform structures of ~10-nm wide and ≥5 μm in length (Fig. 1, C and D). These data infer that proficient maintenance of the trichocyte keratins in strongly reducing conditions is essential for optimal assembly. The apparent quality of IF

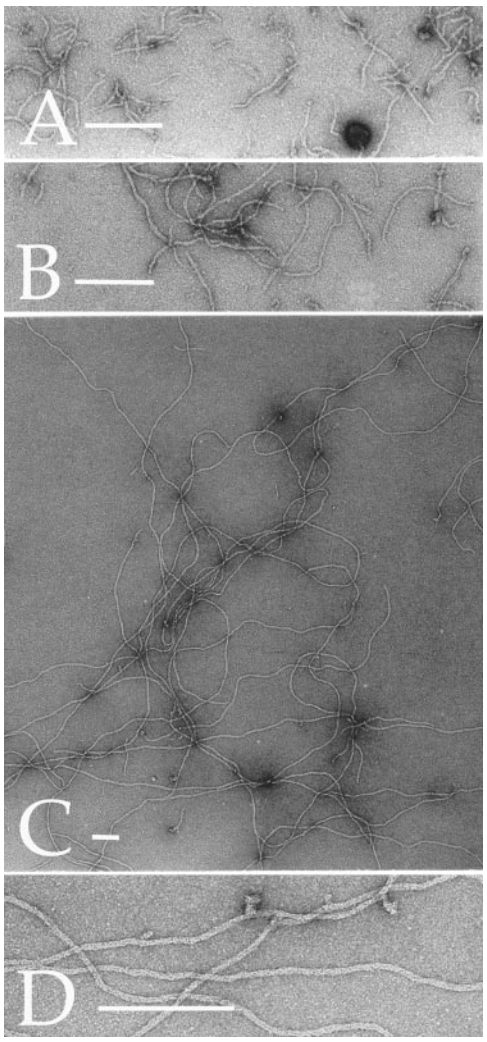

Figure 1. Optimized in vitro assembly of mouse trichocyte keratin IF. Equimolar mixtures of both chains (0.5 mg/ml) were made in 9.5 M urea and dialyzed through a series of decreasing urea concentrations. Final assembly was performed in a buffer of 10 mM Tris-HCl, pH 8.0, 2.5 mM EDTA, 175 mM NaCl, and (A) 5 mM DTT, (B) 5 mM DTT in degassed/N_2-restored buffers, or (C and D) 5 mM TCEP in degassed/N_2-restored buffers. The latter IF are long (>5 μm) smooth-walled structures morphologically indistinguishable from most other types of native or in vitro assembled IF. Negatively stained with 0.7% uranyl acetate. Bars, 0.2 μm.

was not notably affected by 1–5 mM $MgCl_2$ under these optimized conditions. However, keratins recovered from adult mouse hair formed only poor IF structures in H buffer under these optimized conditions, possibly due to protein postsynthetic modifications (data not shown).

At protein concentrations of 0.05–0.5 mg/ml in a buffer of 10 mM Tris-HCl, 25 mM NaCl, 2.5 mM EDTA, and 5 mM TCEP (=L buffer) using optimized conditions, the particles were 50–70-nm long and 2–3-nm wide, suggestive of single molecules or small oligomers thereof (Fig. 2 A). To examine the earliest stages of IF assembly experimentally possible, 1 M NaCl was added to proteins in L buffer to a final concentration of 175 mM, and samples were examined as soon as possible. After ~15 s, the small oligomers had rapidly grown to form raft-like structures of variable width (5–20 nm) and length (75–300 nm) (Fig. 2

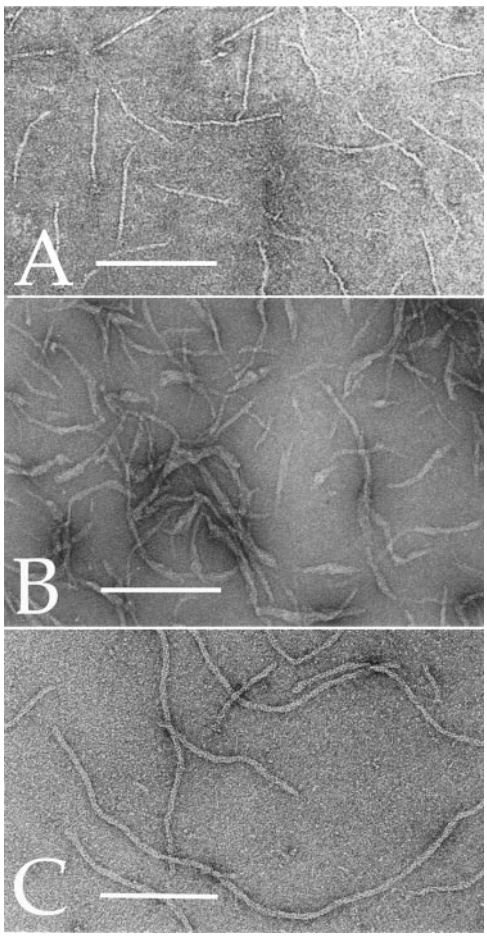

Figure 2. Early stages of trichocyte keratin IF assembly in vitro. (A) Proteins were equilibrated into L buffer at ~40 μg/ml. Only small oligomers are present. (B) Proteins were equilibrated into L buffer at ~0.4 mg/ml, and then made to 175 mM NaCl and sampled 10–15 s later. In this case, a range of particles are seen, ranging from wider raft-like oligomers, half or full-width unit-length IF particles, to short IF of variable width. These images are reminiscent of the data of Herrmann et al. (1999). However, we were unable to obtain more uniform populations of particles at shorter times or at lower protein concentrations, suggesting that trichocyte IF assembly proceeds very rapidly. (C) Same as B, but 1 min after addition of NaCl. At this time, short IF of normal width and smooth appearance are present. Bars, 0.2 μm.

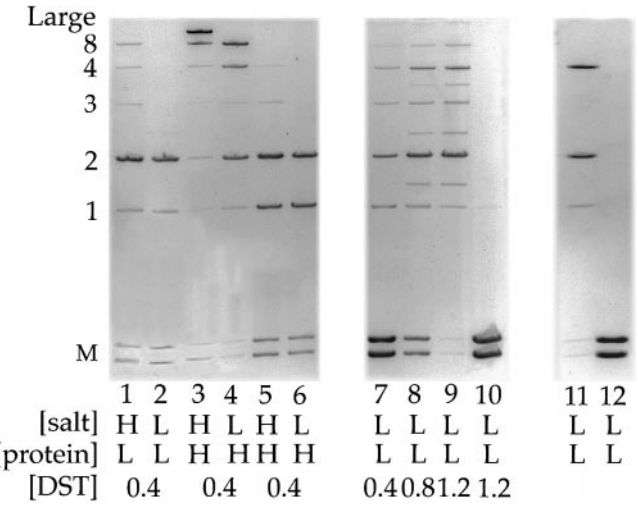

Figure 3. Oligomeric status of in vitro assembled expressed (lanes 1–4 and 7–12) or mouse hair (5 and 6) trichocyte keratins. (Lanes 1–10) Cross linking with DST, (11 and 12) cross linking induced by oxidation with the Cu-P reagent. Equimolar mixtures of the type Ia and IIa chains were equilibrated into assembly buffer containing TCEP in either H (175 mM) or L (25 mM) NaCl concentrations, and either low (L, ≈50 μg/ml) or high (H, 0.5 mg/ml) protein concentrations. (Lanes 7–10) Optimized DST cross-linking concentration, (10) control cleavage reaction of DST–cross-linked material with periodate, and (12) control cleavage of oxidized material with DTT.

B): many particles had raft-like regions 10–20-nm wide on one end with regions that were more uniformly 10-nm wide on the other end. By 1–2 min, all IF particles were fairly uniformly 10-nm wide but 0.4–1-μm long (Fig. 2 C). Together, these data document that, in principle, trichocyte keratin IF assembly follows the same stages as observed for many other IF types, beginning with rapid assembly of small oligomers into "unit length" structures, followed by contraction into 10-nm-wide IF, and finally elongation (Herrmann et al., 1999).

State and Stability of Oligomerization of Trichocyte Keratins during Assembly In Vitro

Cross linking with 0.4–1 mM DST was used to explore the oligomeric status of the reduced and oxidized trichocyte Ia/IIa keratins in L or H assembly buffers. First, 0.4 mM reagent appeared optimal with minimal or no collision-complex formation (Fig. 3, compare lane 7 with lanes 9 and 10). The reduced expressed proteins at low concentration (≤50 μg/ml) in either L or H buffer formed primarily tetramers (two-molecule species), as well as some oligomers up to an apparent eight-molecule size (Fig. 3, lanes 1, 2, and 7). At 400–500 μg/ml, larger oligomers were formed, either too large to enter the separation gel for H buffer (as expected for IF formation, lane 3) or up to eight molecules in size in L buffer (lane 4). After oxidation with the Cu-P reagent, the largest oligomers appeared to be four molecules in size (lane 11). In contrast, keratins recovered from adult mouse hair formed generally smaller oligomers (lanes 5 and 6). Thus, the trichocyte keratins tend to form larger oligomers in solutions of low ionic strength than seen for cytokeratins (Steinert et al., 1993a,b), and are more similar to type IV IF chains (Cohlberg et al., 1995; Steinert et al., 1999).

Samples of isolated bands presumably containing one, two, four, or eight molecules from DST–cross-linked reduced keratins, as well as the two- and four-molecule–sized bands from oxidized keratins were freed of SDS and dialyzed into H assembly buffer. Each of the oligomers from the reduced keratins assembled efficiently into long IF (Fig. 4, A and B, for two- and four-molecule species), indicating that the oligomers were still assembly competent and thus relevant for further structural analyses. On the other hand, the oxidized two- (not shown) or four-molecule (Fig. 4 C) bands formed only subfilamentous particles, the smallest of which appeared like two-molecule oligomers 60–70-nm long. However, they did reassemble if first reduced with 5 mM TCEP (not shown). Thus, the degree of DST modification of lysines could not be the cause

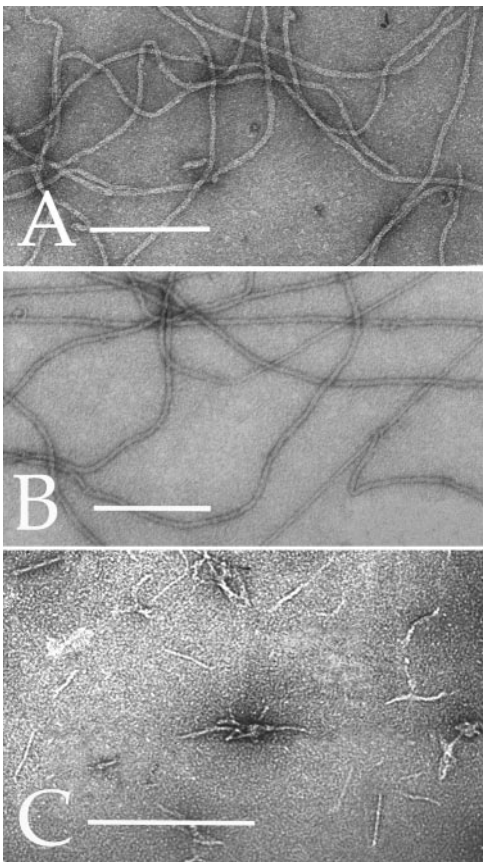

Figure 4. Assembly status of cross-linked oligomers formed in vitro. (A and B) Samples of the two- and four-molecule–sized oligomers from the DST–cross-linking reactions formed normal IF on equilibration under optimized assembly conditions. (C) Samples from the four-molecule oligomer from the oxidized sample formed only small particles, indicating failed IF assembly in vitro. However, after reduction with 5 mM DTT or TCEP, IF assembly proceeded (not shown). Bars, 0.2 μm.

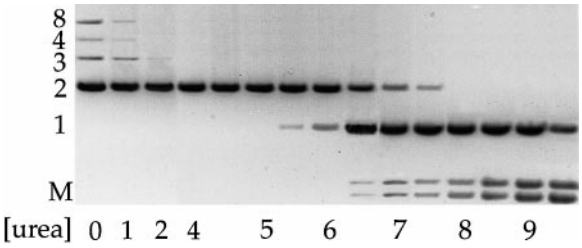

Figure 5. Trichocyte chains form very stable one- and two-molecule entities in vitro. Samples were equilibrated in urea solutions of the concentrations shown and cross linked with 25 mM DST. The urea concentrations at which the two- (~6 M) and one-molecule (~9 M) species dissociate are almost identical to those found for other cytokeratin IFs (Wu et al., 2000).

of failed IF assembly in the oxidized case. An alternative possibility is that molecules in the oxidized oligomers had instead assumed a nonproductive assembly alignment mode that inhibited or interfered with IF assembly.

By cross linking with 25 mM DST in urea solutions of increasing concentrations, we found that the two-molecule (tetramer) and one-molecule (dimer) species of expressed trichocyte chains were stable in 6 and ~8.5 M urea, respectively (Fig. 5), as found for cytokeratins and other IF chain types (Wawersik et al., 1997; Steinert et al., 1999; Wu et al., 2000).

Recovery and Sequences of DST Cross-Linked Reduced Trichocyte Keratin Oligomers

Large-scale cross-linking reactions of expressed trichocyte keratins (≈50 μg/ml in H buffer) were performed, followed by recovery of four sizes of oligomers for CNBr/trypsin cleavage. Fig. 6 shows HPLC chromatograms of resolved peptides. In comparison to unreacted chains (Fig. 6 A), 30 peaks were recovered that contained DST–cross-linked peptides. Of these, five common peaks were due to intramolecular cross linking across the heterodimer molecule, 12 peaks arose in the two-molecule oligomer, another six in the four-molecule oligomer, and seven more in the four-molecule oligomer. Amino acid analyses and protein sequencing for up to 12 Edman degradation cycles allowed identification of the Lys residues involved in each case. Almost all Lys residues on the rod domains of both the types Ia and IIa chains were used, and often with different partners. Most of these were located in identical positions as were found in previous cross-linking studies of cytokeratins vimentin and α-internexin (Steinert et al., 1993a,b,c; 1999), which thereby adds validity to this database. 18 peaks could be assigned confidently to either one of three modes of alignment between antiparallel molecules—A_{11} (7), A_{22} (5), or A_{12} (6)—described previously for other IF types (see Table I and Fig. 8). A total of seven other cross links (Fig. 6 B, 9, 12, 16, 22, 23, 27, and 30) may be due to linkages between molecules four rows apart in a two-dimensional surface lattice and will not be discussed further here.

Recovery and Sequences of Cross-Linked Oxidized Trichocyte Keratin Oligomers

In initial experiments, we examined the one-, two-, and four-molecule oligomers formed by disulfide bond cross linking induced by the Cu-P complex. Under the conditions of oxidation used, >95% of the cysteine-SH groups had become unreactive to iodoacetamide, suggestive of near-complete disulfide bond formation. After protein cleavage, in comparison with the unoxidized proteins, many tryptic peptides reproducibly moved due to oxidation in the one-molecule species, presumably due to formation of intramolecular disulfide bonds (compare Fig. 6, A with C). However, in the two- (not shown) and four-molecule (Fig. 6 D) oligomers, a total of 10 peptides reproducibly shifted again, which were recovered for sequencing. Of these, six disulfide bond links occurred between rod domain cysteines, each of which could be assigned to an established alignment mode. Several of these links have been predicted to occur among trichocyte keratin molecules in vivo (Parry, 1995, 1996). Four other peptides (Fig. 6 D, 5 and 8–10) involved links between head or tail domain and rod domain cysteines.

Nevertheless, these provided insufficient data points to adduce molecular alignment information. Accordingly, these experiments were repeated with the two- (not shown) and four-molecule (Fig. 6 E) bands recovered from the oxidized trichocyte keratin and then cross linked with DST. In this case, 27 peaks were reproducibly recov-

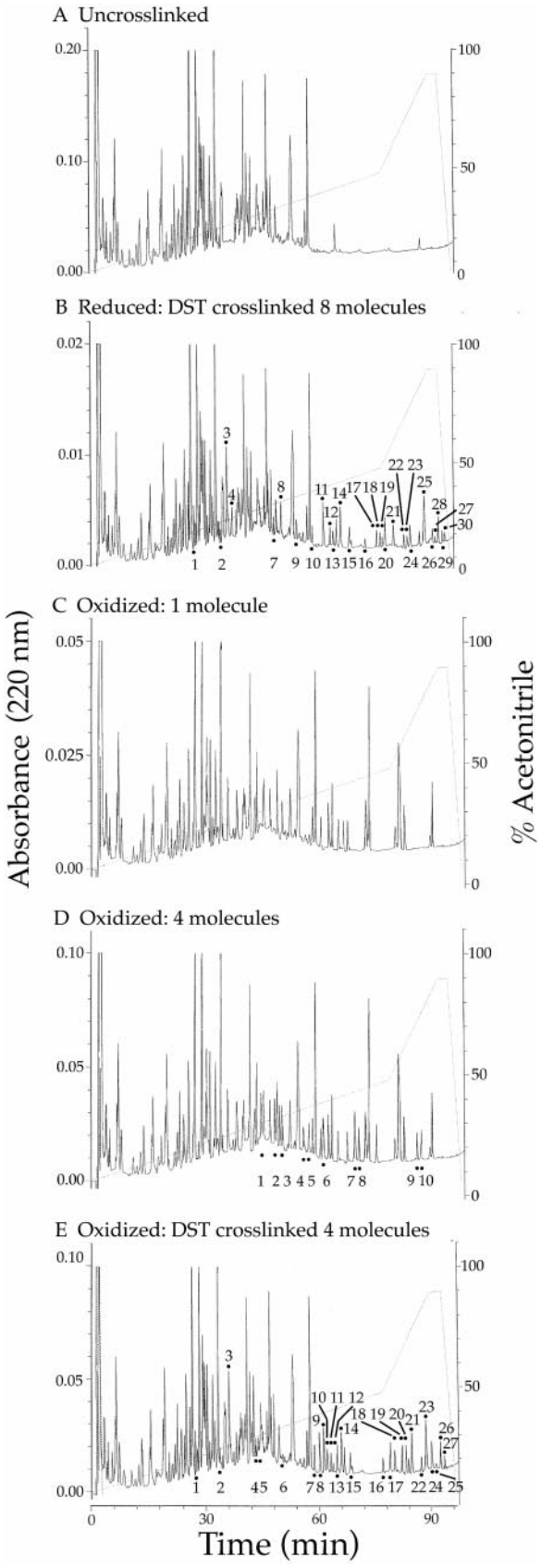

Figure 6. HPLC fractionation of DST–cross-linked CNBr/trypsin cleavage products of trichocyte IF oligomers. Peptide profiles are from the following experiments: (A) unreacted trichocyte chains, (B) DST–cross-linked eight-molecule oligomer from reduced proteins showing 30 peaks used for analyses, (C) oxidized one-molecule oligomer showing numerous shifted peaks due to disulfide bond formation, (D) oxidized four-molecule oligomer showing 10 new peaks used for analyses, and (E) oxidized four-molecule oligomer followed by DST–cross linking showing 25 new peaks used for analyses.

ered from the HPLC profiles and were recovered for sequencing. While most peaks were identical to those of the reduced chains, 11 new peaks indicative of a different A_{11} alignment mode were found.

Calculation of Rod Domain Axial Alignments of Molecules and Linker Segment Lengths

Table I summarizes the data for DST-induced cross links of reduced and oxidized trichocyte IF that were used for calculations. The body of data consist of: eight A_{22} alignments (of which seven are common in the reduced and oxidized sets), seven A_{12} alignments (six common), seven A_{11} alignments unique to the reduced keratins, and 11 A_{11} alignments unique to the oxidized keratins. An additional two, one, and three cross links delineating A_{22}, A_{12}, and A_{11} alignments, respectively, were obtained from the disulfide bond set (Table I). All of the data were subjected to least squares analyses using established methods (Steinert et al., 1993a) to refine the six parameters that define both the molecular (links L1, L12, and L2) and alignment (A_{11}, A_{22}, and A_{12}) parameters. The disposition of the cross links allows the relative axial staggers between coiled-coil segments to be determined with considerable accuracy. However, due largely to an unfavorable disposition of lysine residues in the protein sequences, the recovered cross links do not fall into positions that allow the linkers L12 and L2 to be specified and, to a large extent, L1 as well. For this reason, these linkers were set to the values determined for the cytokeratins, where the cross links do fall in positions that allow the axial extent of the linkers to be determined. This approach seems justified for linkers L12 and L2 on the grounds that the primary structures of the cytokeratin and trichocyte keratins have a very high degree of sequence identity (and close to 100% homology) for both linkers (Fig. 7). However, the evidence that the axially projected molecular length of linker L1 is the same is not as clear-cut since the degree of sequence homology is modest. As a result, the calculations were performed in two ways: (a) with all linker lengths held constant at the cytokeratin values, and (b) with only L12 and L2 lengths held constant at the cytokeratin values. In general, the results were similar. The refined values (Table II) show that the parameters calculated for reduced trichocyte keratins are similar to those determined for cytokeratins. In the case of the oxidized keratins, the values for A_{12} and A_{22} and the link L1 were also similar to those of the reduced trichocyte keratins and cytokeratins, but the value for A_{11} revealed a shift forward by ~15 residues, resulting in a 2-nm increase of net molecular repeat length. Alignment of pairs of molecules (Fig. 8) thus reveals that, whereas there is a small head-to-tail overlap of about six residues in the A_{CN} mode in reduced trichocyte IF, there is a gap of 10–15 residues in the oxidized IF. Moreover, the axial values for the trichocyte keratins oxidized in vitro are remarkably similar to those modeled from earlier x-ray diffraction analyses of well-ordered IF of wool (Table II).

Table I. Unique Intermolecular Cross Links Used in the Least-Squares Analyses and Determination of the Equations Used for Each

Cross link		Fig. 6 peak No.	A12	A11	A22	L1	L12	L2	Value*
Reduced trichocyte DST cross links									
II	1A-05–II 2B-04‡	6B 2	0	1	0	0	0	0	−112
II	1A-31–II L12-10§	6B 14	0	1	0	0	0.41	1	−120
I	1B-33–II 1B-62	6B 16	0	1	0	−1	1	1	−112
II	1B-40–II 1B-61	6B 4	0	1	0	−1	1	1	−106
II	1B-40–II 1B-62	6B 17	0	1	0	−1	1	1	−105
II	1B-41–II 1B-61	6B 6	0	1	0	−1	1	1	−105
II	1B-42–II 1B-61	6B 7	0	1	0	−1	1	1	−104
II	1A-05–II 2B-120	6B 18	1	0	0	0	0	0	3
I	1B-33–II 2B-49	6B 26	1	0	0	−1	0	0	−5
II	1B-40–II 2B-44	6B 5	1	0	0	−1	0	0	−3
I	1B-42–II 2B-44	6B 8	1	0	0	−1	0	0	−1
I	1B-71–II 2B-09	6B 19	1	0	0	−1	0	0	−7
II	L1-04–II 2B-83§	6B 10	1	0	0	−0.4	0	0	−1
II	2B-04–I 2B-120	6B 11	0	0	1	−1	−1	−1	157
II	2B-09–II 2B-120	6B 13	0	0	1	−1	−1	−1	162
I	2B-10–I 2B-120	6B 29	0	0	1	−1	−1	−1	163
II	2B-44–II 2B-81	6B 15	0	0	1	−1	−1	−1	158
II	2B-49–II 2B-71	6B 21	0	0	1	−1	−1	−1	153
Oxidized trichocyte DST cross links									
I	1B-17–II 1B-66	6D 1	0	1	0	−1	1	1	−124
I	1B-70–II 1B-17	6D 4	0	1	0	−1	1	1	−120
I	1B-87–I L1-09	6D 6	0	1	0	−0.82	1	1	−120
I	1B-101–I 2A-11	6D 3	1	0	0	−1	0	1	6
II	2B-05–I 2B-119	6D 2	0	0	1	−1	−1	−1	157
I	2B-22–I 2B-105	6D 7	0	0	1	−1	−1	−1	160
Oxidized trichocyte novel DST cross links‖									
II	1A-01–II 2A-10	6E 16	0	1	0	0	0	1	−130
II	1A-05–II 2A-10	6E 12	0	1	0	0	0	1	−126
I	1A-17–II L12-10	6E 8	0	1	0	0	0.41	1	−124
II	1A-17–II L12-10	6E 14	0	1	0	0	0.41	1	−124
I	1B-14–I 1B-71	6E 21	0	1	0	−1	1	1	−122
I	1B-14–II 1B-71	6E 25	0	1	0	−1	1	1	−122
I	1B-19–II 1B-62	6E 19	0	1	0	−1	1	1	−126
II	1B-40–I 1B-42	6E 4	0	1	0	−1	1	1	−125
II	1B-41–I 1B-42	6E 5	0	1	0	−1	1	1	−124
I	1B-42–I 1B-42	6E 10	0	1	0	−1	1	1	−123
I	1B-89–II L1-04	6E 20	0	1	0	0.4	1	1	−118

*The values relating to each cross-link position were calculated using standard equations and are expressed in terms of h_{cc}, the average linear rise of a single residue in a coiled-coil, which is 0.1485 nm. ‡For example, for the cross link between positions 1A-05 and 2B-04 in the type II chain, the equation is (0 × A12) + (A11) + (A22) − (L1) + (L12) + (L2) = −112. §Fractional numbers can occur in equations involving the linker sequences because the cross-link data reveal that the average linear rise for each residue in the linker segments is <0.1485 nm. ‖Almost all of the intermolecular linkages for the A12 (Fig. 6 E, peaks 2, 6, 7, 17, and 24) and A22 (peaks 9, 11, 13, 15, 19, and 27) alignment modes are the same as for the reduced set and are not listed again.

Discussion

The extant published literature on the structure aspects of trichocyte keratin (hard α-keratin) contains a variety of observations and ideas, some of which seem (at first sight) to be mutually incompatible. Significantly, all of the IF types studied thus far using cross-link technology (K1/K10 and K5/K14 cytokeratins, vimentin, α-internexin) have been shown to contain parallel molecules with a head-to-tail overlap of about eight residues (Steinert et al., 1993a,b,c, 1999). In contrast, Parry (1995, 1996) has documented that parallel molecules in trichocyte keratin display a head-to-tail gap of ~10 residues (1 nm) instead. But there are two issues unique to trichocyte IF. First, the measured axial repeat in trichocyte keratin, determined from x-ray diffraction of well-oriented specimens of wool (47 nm; Fraser and MacRae, 1983, 1985; Fraser et al., 1986) is clearly larger than that calculated from cross link (45 nm, Steinert et al., 1993a) or shadowing (45.4 nm; Steven et al., 1985) studies on cytokeratins. Construction of a two-dimensional surface lattice of the molecular organization in trichocyte IF demonstrated that the A_{11} mode of alignment in particular was shifted forward by 1–2 nm in comparison with that of the cytokeratins, thereby resulting in a longer axial molecular repeat as well as an apparent head-to-tail gap. However, one early but unsubstantiated x-ray diffraction study reported that the molecular repeat length of IF in wool follicles was less than that in the mature wool fiber itself (Dobb et al., 1965). Second, unlike cytokeratins, trichocyte keratins possess several cysteine residues in their rod domain segments. Assuming that these cysteines pair to form disulfide, the maximal number of disulfides could theoretically occur between molecules aligned as predicted from the surface lattice deduced by x-ray diffraction (Fraser et al., 1988; Parry, 1995, 1996); that is, in which the A_{11} alignment mode is shifted forward in comparison to cytokeratins. The formation of these disulfide bonds would contribute a high degree of stability to the trichocyte IF and should provide precisely the features re-

Table II. Axial Parameters for Cytokeratins, and Reduced and Oxidized Trichocyte Keratins, Deduced from Antiparallel Cross-link Data

		Reduced trichocyte		Oxidized trichocyte		
	K1/5/10/14	All linkers fixed	Only L12 and L2 fixed	Model*	All linkers fixed	Only L12 and L2 fixed
Repeat	304.44	305.07	302.60	316.60	322.37	319.61
Overlap	6.83	6.20	0.02	−9.09	−11.10	−17.10
A12	0.43	9.10	2.76	6.38	11.11	3.40
A11	−111.62	−111.20	−117.38	−126.92	−128.35	−134.35
A22	192.82	193.87	185.22	189.68	194.02	185.26
L1	16.27	16.27	7.62	12.51	16.27	7.51
L12	13.94	13.94	13.94	13.94	13.94	13.94
L2	5.06	5.06	5.06	5.06	5.06	5.06
Δz (1BU, 1BD)	−3.89	−3.47	−1.00	−15.43	−20.62	−17.86
Δz (2BU, 2BD)	2.56	3.60	3.60	3.17	3.75	3.75
Δz (1BU, 2D)	−50.84	−42.17	−39.87	−41.13	−40.16	−39.11

*Parry (1995).

quired to serve their designated mechanical role in vivo. Thus, these considerations appear teleologically attractive and are consistent with the known physical (hardened) properties of tissues that contain trichocyte IF. Disulfide-bond stabilization is also known to occur in IF of other terminally differentiated epithelia such as the cytokeratin K1/K10 chains in the epidermis (Steinert and Parry, 1993) or K4/K13 chains in the esophagus (Pang et al., 1993). In these cases, however, only one or two disulfide bonds are likely formed between cysteines on rod-domain segments (Steinert and Parry, 1993).

Thus, why are the trichocyte keratins of mature tissues structurally different from other members of the IF family? The sequences that are believed to be involved in the head-to-tail overlap (i.e., the helix initiation motif at the beginning of segment 1A and the helix termination motif at the end of segment 2B) are highly conserved across the entire family of IF chains, including those from trichocyte keratins. Furthermore, mutations in trichocyte keratin chains that cause monilethrix, a genetic disease of hair fiber formation, occur either in the 1A segment (Asn8His and Asn8Asp in the hHb6 chain) or the 2B segment (Glu117Lys and Glu117Asp in the hHb6 chain and Glu106Lys and Glu117Lys in the hHb1 chain; see Korge et al., 1999). These correspond to the two "hot spots" in cytokeratin chains in which mutations commonly lead to keratinopathies (Korge and Krieg, 1996; Irvine and McLean, 1999). Why, therefore, does a mutation in trichocyte keratin at this point result in a disease state when the head-to-tail overlap in which it would be expected to play an important role is clearly absent in the hair? In addition to these data, we (data not shown) and Herrling and Sparrow (1991) have shown that cytokeratin and trichocyte keratin chains can copolymerize and thus form type Ia/IIb and Ib/IIa molecules and small oligomers. Likewise, trichocyte keratins expressed after transfection into cultured keratinocytes assemble onto the existing cytokeratin IF networks (Yu et al., 1991). Together, these data suggest that molecular parameters (including link lengths) should be very similar or identical.

The questions that this study has attempted to answer are therefore as follows: which data are correct? and can a rationalized model be proposed? The answers provided below are remarkable for they show that the published data are not only correct, but self-consistent. They fit to-

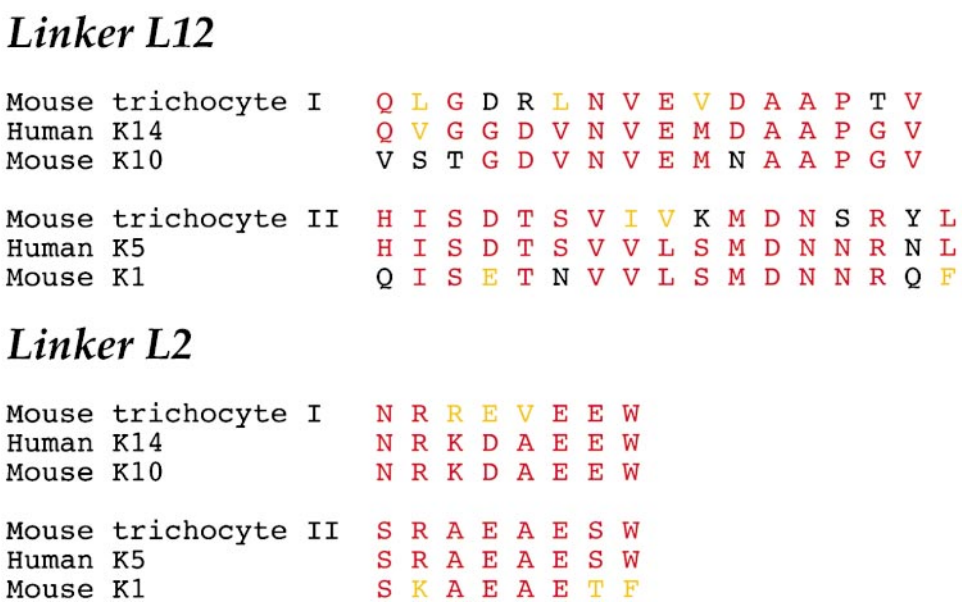

Figure 7. High homology among the sequences of the L12 and L2 linker segments for trichocyte keratins and cytokeratins. (Red) Identical residues, and (orange) homologous residues. Based on these similarities, calculations were based on the reasonable assumption that the linker segments of the two systems may have similar axial lengths.

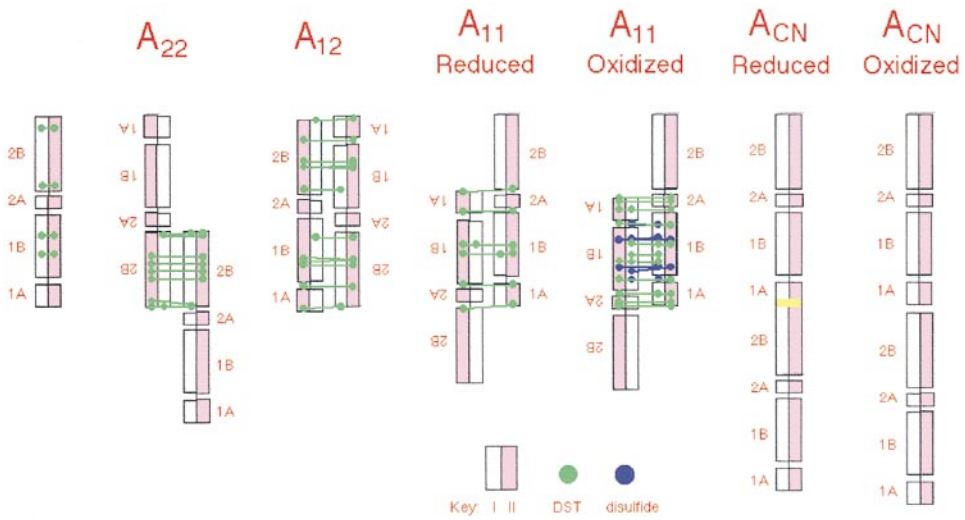

Figure 8. Molecular alignments in trichocyte keratin IF based on calculations of the DST and oxidative cross linking. The models are built from the data of Table II. Note: the yellow region represents the predicted overlap in the reduced A_{CN} mode.

gether into a simple model involving a disulfide-bond–stabilizing molecular rearrangement in trichocyte keratin IF during terminal differentiation in the tissues.

Reassembly of Mouse Trichocyte IF In Vitro in High Yield

In vitro assembly of trichocyte keratin IF has proved difficult to achieve. Early work on the reconstitution of wool keratin IF (Conrads et al., 1988), for example, was not easily reproduced. However, Heid et al. (1988) and Winter et al. (1997) have made progress using mouse proteins in preference to those of sheep wool. We can now report that mouse trichocyte IF can be assembled reproducibly in vitro in high yield and of apparent clean morphological quality using appropriate reducing and near physiological buffer conditions. Visually, these IF appear morphologically identical to the native IF recovered from rat vibrissae (Jones and Pope, 1985; Jones et al., 1997).

This has permitted for the first time a direct in vitro analysis of the axial parameters and molecular alignments of trichocyte IF. The values adduced for reduced trichocyte oligomers (Table II) are, within the limits imposed by the disposition of lysine residues in the proteins, identical to those obtained for cytokeratins.

The A_{11} Molecular Alignment Mode Differs between Reduced and Oxidized Trichocyte Keratin Oligomers

Next we sought methods to evaluate these parameters in IF oxidized in vitro with the Cu-P reagent. We could achieve >95% oxidation of the cysteine–SH groups and, further, we recovered reproducible HPLC patterns of resolved CNBr/tryptic peptide peaks both before and after DST cross linking, suggesting that there was a preferred pattern of disulfide bond formation in solution. While the A_{12} and A_{22} modes of alignment were the same as those of reduced trichocyte keratins and cytokeratins, the A_{11} alignment mode was shifted by ~15 residues, resulting in an increased net axial length of ~2 nm (Table II). Remarkably, the resulting axial values and molecular parameters match closely those deduced earlier by Parry (1995, 1996) from the x-ray diffraction data of Fraser and MacRae (1983, 1985) and Fraser et al. (1986). Furthermore, the resulting two-dimensional surface lattice of molecular organization closely fits that adduced from the x-ray diffraction data of wool. Moreover, in the in vitro–oxidized IF, six disulfide bonds were induced between cysteine residues in adjacent antiparallel rod domain segments. These correspond exactly to those predicted by Parry (1995, 1996) based on the earlier x-ray diffraction data. Thus the solution oxidation experiments performed here have mimicked to a marked degree the disulfide bonding events that occur in vivo.

Hypothesis: An Oxidation-dependent Molecular Shift Stabilizes Trichocyte IF on Terminal Differentiation of the Hair Cortical Cell

The conclusion from this work is quite simple. It is known that the synthesis and assembly of trichocyte keratin molecules into IF occurs in a reducing environment in, for example, the columns of cortical cells located immediately above the dermal papilla of the hair follicle (Langbein et al., 1999). The hair matrix (IFAP) proteins are deposited and interdigitate with the IF at a later stage toward the end of IF synthesis (reviewed in Fraser et al., 1972). Only much later, further up the hair follicle during terminal differentiation and cell death, does the cellular environment change to an oxidizing one where disulfide bond formation occurs. Our data document that there is a head-to-tail overlap of molecules in trichocyte IF initially assembled in a reducing environment in the cells. This therefore appears to be an important and common feature of the assembly process of all IF types and, further, any inappropriate amino acid substitutions that occur in the overlap region as, for example, those observed in monilethrix, jeopardize successful assembly. These molecular alignments for reduced trichocyte keratins demonstrate that two or three pairs of cysteine residues lie in appropriate positions that theoretically could form disulfide bonds. However, upon oxidation, we identified 10 disulfide bonds, including six between rod domain cysteines that were all predicted in earlier analyses (Parry, 1995, 1996). These disulfide bonds reflect a molecular shift of primarily only the A_{11} alignment mode. We believe that this molecular shift occurs to maximize the number of stabilizing intermolecular disulfide bonds. This would have the net effect of significantly strengthening the trichocyte IF structure and the tissue containing them. These considerations therefore offer a novel role for disulfide bonds in stabilizing IF.

Finally, it is of interest to speculate on the molecular biomechanics of the A_{11} alignment shift induced by oxidation/disulfide bond formation. In addition to the six disulfide bonds formed between rod domain cysteines, we also recovered four disulfide bond links between head domain and rod domain cysteines. A large body of literature in various IF systems has documented an absolute requirement of head domain sequences for IF assembly and stability (reviewed in Fuchs and Weber, 1994; Parry and Steinert, 1995), which is presumably also the case for trichocyte keratin IF. However, in this case, at least some of the head domain cysteine residues may be positioned so that, upon oxidation, a number of disulfide bonds form that promote a cascade phenomenon to form a series of maximally stabilizing intermolecular disulfide bonds between rod domain cysteines, and thereby impose a shift of the A_{11} molecular mode. This shift may be akin to "tetramer switching" (Steinert, 1991; Herrmann and Aebi, 1998). However, we cannot formally exclude the possibility in intact tissues that disulfide bonding between IFAP proteins may also contribute to or even cause such shifts, and that sulfhydryl oxidases may facilitate the process. Nevertheless, discovery of this novel stabilization role for disulfide bonding suggests that further detailed analyses of the interactions of head and rod domain sequences of trichocyte keratins may provide new information on the higher-order structures of IF in general.

We thank Drs. Bruce Fraser and Helmut Zahn for their insightful comments and unwavering intellectual support during the course of this project.

Submitted: 7 July 2000
Revised: 26 October 2000
Accepted: 30 October 2000

References

Baird, B.A., and G.G. Hammes. 1976. Chemical cross-linking studies of chloroplast coupling factor 1. *J. Biol. Chem.* 251:9653–9662.

Bertolino, A.P., D.M. Checkla, R. Notterman, I. Sklaver, T.A. Schiff, I.M. Freedberg, and G.J. DiDona. 1988. Cloning and characterization of a mouse type I hair keratin cDNA. *J. Invest. Dermatol.* 91:541–546.

Cohlberg, J.A., H. Hajarian, T. Tran, P. Alipourjeddi, and A. Noveen. 1995. Neurofilament protein heterotetramers as assembly intermediates. *J. Biol. Chem.* 270:9334–9339.

Conrads, A., H. Thomas, K.H. Phan, H. Zahn, and H. Hocker. 1988. In vitro reconstitution of nail intermediate filaments. *Naturwissenschaften.* 75:100–101.

Dobb, M.G., R.D.B. Fraser, and T.P. MacRae. 1965. The structure of the keratin filament. *Proceedings of the Third International Wool Textile Conference.* 1:95–102.

Fraser, R.D.B., and T.P. MacRae. 1983. The structure of the α-keratin microfibril. *Biosci. Rep.* 3:517–525.

Fraser, R.D.B., and T.P. MacRae. 1985. Intermediate filament structure. *Biosci. Rep.* 5:573–579.

Fraser, R.D.B., T.P. MacRae, and A. Miller. 1964. The coiled-coil model of α-keratin structure. *J. Mol. Biol.* 10:147–156.

Fraser, R.D.B., T.P. MacRae, and G.E. Rogers. 1972. Keratins, Their Composition, Structure and Biosynthesis. C.C. Thomas, Springfield, IL.

Fraser, R.D.B., T.P. MacRae, D.A.D. Parry, and E. Suzuki. 1986. Intermediate filaments in α-keratins. *Proc. Natl. Acad. Sci. USA.* 83:1179–1183.

Fraser, R.D.B., T.P. MacRae, L.G. Sparrow, and D.A.D. Parry. 1988. Disulphide bonding in α-keratin. *Int. J. Biol. Macromol.* 10:106–112.

Fuchs, E., and K. Weber. 1994. Intermediate filament structure, dynamics, function, and disease. *Annu. Rev. Biochem.* 63:345–382.

Hatzfeld, M., and W.W. Franke. 1985. Pair formation and promiscuity of cytokeratins: formation in vitro of heterotypic complexes and intermediate filaments by homologous and heterologous recombinations of purified polypeptides. *J. Cell Biol.* 101:1826–1841.

Heid, H.W., I. Moll, and W.W. Franke. 1988. Patterns of expression of trichocytic and epithelial cytokeratins in mammalian tissues. I. Human and bovine hair follicles. *Differentiation.* 37:137–157.

Herrling, J., and L.G. Sparrow. 1991. Interactions of intermediate filament proteins from wool. *Int. J. Biol. Macromol.* 13:115–119.

Herrmann, H., and U. Aebi. 1998. Intermediate filament assembly: fibrillogenesis is driven by decisive dimer–dimer interactions. *Curr. Opin. Struct. Biol.* 8:177–185.

Herrmann, H., M. Häner, M. Brettel, S.A. Müller, K.N. Goldie, B. Fedtke, A. Lustig, W.W. Franke, and U. Aebi. 1996. Structure and assembly properties of the intermediate filament protein vimentin: the role of its head, rod and tail domains. *J. Mol. Biol.* 264:933–953.

Herrmann, H., M. Häner, M. Brettel, N.O. Ku, and U. Aebi. 1999. Characterization of distinct early assembly units of different intermediate filament proteins. *J. Mol. Biol.* 286:1403–1420.

Irvine, A.D., and W.H.I. McLean. 1999. Human keratin diseases: the increasing spectrum of disease and subtlety of the phenotype-genotype correlation. *Br. J. Dermatol.* 140:815–828.

Jones, L.N., and F.M. Pope. 1985. Isolation of intermediate filament assemblies from human hair follicles. *J. Cell Biol.* 101:1569–1577.

Jones, L.N., M. Simon, N.R. Watts, F.P. Booy, A.C. Steven, and D.A.D. Parry. 1997. Intermediate filament structure: hard α-keratin. *Biophys. Chem.* 68:83–93.

Konigsberg, W.H., and L. Henderson. 1983. Removal of sodium dodecyl-sulfate from proteins by ion-pair extraction. *Methods Enzymol.* 91:254–259.

Korge, B.P., and T. Krieg. 1996. The molecular basis for inherited bullous diseases. *J. Mol. Med.* 74:59–70.

Korge, B.P., H. Hamm, C.S. Jury, H. Traupe, A.D. Irvine, E. Healy, M. Birch-MacHin, J.L. Rees, A.G. Messenger, S.C. Holmes, D.A.D. Parry, and C.S. Munro. 1999. Identification of novel mutations in basic hair keratins hHb1 and hHb6 in monilethrix: implications for protein structure and clinical phenotype. *J. Invest. Dermatol.* 113:607–612.

Langbein, L., M.A. Rogers, H. Winter, S. Praetzel, U. Beckhaus, H.R. Rackwitz, and J. Schweizer. 1999. The catalog of human hair keratins. I. Expression of the nine type I members in the hair follicle. *J. Biol. Chem.* 274:19874–19884.

Pang, Y.-S.S., A. Schermer, J. Yu, and T.-T. Sun. 1993. Suprabasal change and subsequent formation of disulfide-stabilized homo- and hetero-dimers of keratins during esophageal epithelial differentiation. *J. Cell Sci.* 104:727–740.

Parry, D.A.D. 1995. Hard α-keratin IF: a structural model lacking a head-to-tail molecular overlap but having hybrid features characteristic of both epidermal keratin and vimentin IF. *Prot. Struct. Funct. Genet.* 22:267–272.

Parry, D.A.D. 1996. Hard alpha-keratin intermediate filaments: an alternative interpretation of the low-angle equatorial x-ray diffraction pattern, and the axial disposition of putative disulphide bonds in the intra- and inter-protofilamentous networks. *Int. J. Biol. Macromol.* 19:45–50.

Parry, D.A.D., and P.M. Steinert. 1995. The Structure and Function of Intermediate Filaments. E. Landis Publishing Company, Austin, TX.

Parry, D.A.D., and P.M. Steinert. 1999. Intermediate filaments: molecular architecture, dynamics, assembly and polymorphism. *Q. Rev. Biophys.* 32:99–187.

Steinert, P.M. 1991. Organization of coiled-coil molecules in native keratin 1/keratin 10 intermediate filaments: evidence for alternating rows of antiparallel in-register and antiparallel staggered molecules. *J. Struct. Biol.* 107:157–174.

Steinert, P.M., and D.A.D. Parry. 1993. The conserved H1 subdomain of the type II keratin 1 chain plays an essential role in the alignment of nearest-neighbor molecules in mouse and human keratin 1/keratin 10 intermediate filaments at the two- to four-molecule level of structure. *J. Biol. Chem.* 268:2878–2887.

Steinert, P.M., W.W. Idler, and S.B. Zimmerman. 1976. Self-assembly of bovine epidermal α-keratin. *J. Mol. Biol.* 108:547–567.

Steinert, P.M., L.N. Marekov, R.D.B. Fraser, and D.A.D. Parry. 1993a. Keratin intermediate filament structure: crosslinking studies yield quantitative information on molecular dimensions and mechanism of assembly. *J. Mol. Biol.* 230:436–452.

Steinert, P.M., L.N. Marekov, and D.A.D. Parry. 1993b. Conservation of the structure of keratin intermediate filaments: molecular mechanism by which different keratin molecules integrate into pre-existing keratin intermediate filaments during differentiation. *Biochemistry.* 32:10046–10056.

Steinert, P.M., L.N. Marekov, and D.A.D. Parry. 1993c. Diversity of intermediate filament structure: evidence that the alignment of coiled-coil molecules in vimentin is different from that in keratin intermediate filaments. *J. Biol. Chem.* 268:24916–24925.

Steinert, P.M., L.N. Marekov, and D.A.D. Parry. 1999. Molecular parameters of type IV α-internexin and type IV-type III α-internexin-vimentin copolymer intermediate filaments. *J. Biol. Chem.* 274:1657–1668.

Steven, A.C., R. Stall, P.M. Steinert, and B.L. Trus. 1985. Computational straightening of images of curved macromolecular helices by cubic spline interpolation facilitates structural analysis by Fourier methods. *Proceedings of the Forty-third Annual Meeting Electron Microscopy Association of America.* 7:738–739.

Wawersik, M., R.D. Paladini, E. Noensie, and P.A. Coulombe. 1997. A proline residue in the alpha-helical rod domain of type I keratin 16 destabilizes keratin heterotetramers. *J. Biol. Chem.* 272:32557–32565.

Weinberg, W.C., L.V. Goodman, C. George, D.L. Morgan, S. Ledbetter, S.H. Yuspa, and U. Lichti. 1993. Reconstitution of hair follicle development in vivo: determination of follicle formation, hair growth, and hair quality by dermal cells. *J. Invest. Dermatol.* 100:229–236.

Winter, H., I. Hofmann, L. Langbein, M.A. Rogers, and J. Schweizer. 1997. A splice site mutation in the gene of the human type I hair keratin results in the expression of tailless keratin isoform. *J. Biol. Chem.* 272:32345–32352.

Wu, K.C., J.T. Bryan, M.I. Morasso, S.-J. Jang, J.-H. Lee, J.-M. Yang, L.N. Marekov, D.A.D. Parry, and P.M. Steinert. 2000. Coiled-coil trigger motifs in the 1b and 2B rod domain segments are required for the stability of keratin intermediate filaments. *Mol. Biol. Cell.* 11:3539–3558.

Woods, E.F., and A.S. Inglis. 1984. Organization of the coiled-coils in the wool microfibril. *Int. J. Biol. Macromol.* 6:277–283.

Yu, D.-W., S.-Y. Pag, D.M. Checkla, I.M. Freedberg, T.-T. Sun, and A.P. Bertolino. 1991. Transient expression of mouse hair keratins in transfected HeLa cells: interactions between "hard" and "soft" keratins. *J. Invest. Dermatol.* 97:354–363.